Egypt. J. Chem. **Vol. 64**, No. 10 pp. 5781 – 5792 (2021)

Egyptian Journal of Chemistry

http://ejchem.journals.ekb.eg/

Antibacterial and Antifungal Activity of Green-synthesized Silver Nanoparticles Using *Spinacia oleracea* leaves Extract

Alsayed E. Mekky[1], Ayman A. Farrag[1, 2], Ahmed A. Hmed[1] and Ahmed R. Sofy[1]

[1]*Botany and Microbiology Department, Faculty of Science, Al-Azhar University, Nasr City 11884, Cairo, Egypt*

[2]*Director of Al-Azhar Center for Fermentation Biotechnology and Applied Microbiology, Al-Azhar University, Nasr City 11884, Cairo, Egypt*

Abstract

In this study, silver nanoparticles (AgNPs) were green synthesized using aqueous leaf extracts of green spinach that have been used as antimicrobial agents. The antimicrobial efficacy was evaluated against bacterial and fungal strains. The morphological structures, optical and surface properties of as-synthesized nanoparticles have been investigated via a Transmission electron microscope, X-ray diffraction, UV-Vis absorption, and Fourier transform infrared, respectively. The colloidal stability was evaluated using dynamic light scattering and zeta-potential measurements. The average size of as-synthesized particles was about 15±5nm. The green synthesized AgNPs showed significant antibacterial activity against different bacterial species via the agar well diffusion assay. The inhibition zones were varied from 27 to 34mm against 6 bacterial species (*K. pneumoniae, E.coli, A. baumannii, P. aeruginosa, S. aureus*, and *S. haemolyticus*). In such a case, the minimal inhibition concertation of AgNPs against bacterial isolates was 4µg/ml for all isolates, except *E.coli* was 8µg/ml. Also, the silver particles showed an antifungal behavior against 4 fungal species (*A. niger, P. marneffie, C. glabrata and C. parapsilosis*) with an inhibition zone from 19 to 39mm in diameter. Whereas, the MICs for fungal isolates 8µg/ml for all isolates. Treated Wi-38 cells with AgNPs demonstrated various levels of cytotoxicity dependent on the concentration of AgNPs using MTT assay with IC_{50} ~ 447.6. Moreover, the current study presents a facile and cost-effective synthesis of AgNPs via green chemical methods to be used as antimicrobial agents. Further *in-vivo* assessment is required to evaluate their therapeutic efficacy against MDR microorganisms.

Keywords:Silver nanoparticles, *Spinacia oleracea*, nanoparticles characters, antibacterial and antifungal activities

1. Introduction

In recent decades, nanomaterials gained a great interest in a wide range of applications in all fields of life, from health care to industrial applications, due to their unique physicochemical properties that are related to their size and shape [1-3].

Therefore, several studies have been devoted to develop many drugs based on nano-formulations for fighting the continuous increase in the number of multi-drug resistant bacterial (MDR) and viral strains due to mutation, pollution, and changing environmental conditions [3-7]. In this regard, metal ions, and metallic nanoparticles (NPs) were used to inhibit the growth of many infectious bacteria [8, 9]. Silver (Ag) is one of the best antimicrobial agents from time immemorial [10].

Metallic nanostructures especially AgNPs have considerable interest due to their unique electrical, optical, thermal properties and higher surface-to-volume ratio with the promise of potential claims in optoelectronic devices, catalysis, biosensors, composite materials, cosmetic products, and antimicrobial applications [11-13].

Also, AgNPs are used to inhibit the growth of a variety of pathogenic bacteria in the human system [14]. Moreover, AgNPs are using in the sterilization of catheters, cuts, burns, and wounds against any infection [15].

In the context of a healthy ecological world, there is a growing need for the environment-friendly, green synthesis of the nanoparticles and their systems of the metal nanoparticles, etc [4, 16, 17]. Silver

*Corresponding author e-mail: mekkysayed26@gmail.com
Receive Date: 28 April 2021, Revise Date: 19 May 2021, Accept Date: 23 May 2021
DOI: 10.21608/EJCHEM.2021.74432.3673

nanoparticles have been used broadly in the form of antimicrobial agents in the food industry, textile composition, and many environmental applications [18-20]. The colloidal silver solutions are possessed low toxicity to human cells, high thermal stability, and low volatility, due to these properties, AgNPs are becoming prime materials for medicines, various industries, animal husbandry, accessories, health, and military. AgNPs demonstrate prospective antimicrobial effects against infectious organisms such as *E. coli*, *B. subtilis*, and many more [21].
AgNPs demonstrated highly efficient antifungal; in addition, highly antibacterial activities even against multi-drug resistant bacteria (MDR) species [22].

In a green synthesis of nanomaterials using plant extracts, enzymes, proteins, flavonoids, and other biomolecules exist in the ethanolic or aqueous solutions of these extracts can be utilized as individually or dual effect as reducing and capping agents in the synthetic process of nanoparticles [23].

Comparable to analogous nanostructures, the physicochemical properties of Ag NPs are influenced by any tailoring in their size and shape, which depends on the chemical composition and functional groups that exist in the plant extract [11]. Green synthesis of silver nanoparticles is favored over chemical and physical methods as it is cost-effective, eco-friendly and also nontoxic material [24].

Herein, silver nanoparticles have been green synthesized using *Spinacia Oleracea* leaves extract that is available in the Egyptian markets. In addition, the antimicrobial against pathogenic bacterial and fungal isolates and also cytotoxicity will be investigated.

2. Experimental Section

2.1. Materials

Silver nitrate ($AgNO_3$, 99%) pursued from Sigma-Aldrich, Whatman filter paper. All glasswares were washed with sterile distilled water many times and dried in an oven before use to remove any residual contaminants. Muller-Hinton agar, Nutrient Agar medium**.** Nutrient Broth medium, Potato Dextrose Agar (PDA), and Potato Dextrose Broth (PDB)**,** from Sigma Aldrich- Germany**.**

2.2. Tested microorganisms

Bacteria: Six isolates *Klebsiella pneumoniae, Escherichia coli, Acinitobacter baumannii, Pseudomonas aeruginosa, Staphylococcus aureus,* and *Staphylococcus haemolyticus* isolated from clinical samples, identified depending on cultural, morphological and biochemical analysis according to Bergey's manual [25]. Moreover Vitek2 system was performed to confirm the identification.

Fungi/Yeast: Four isolates were *Aspergilus niger, Penicillium marneffie, Candida glabrata,* and *Candida parapsilosis* isolated from clinical samples and identified at Mycology Laboratory of the Botany and Microbiology Department, Faculty of Science (Boys), Al-Azhar University, Cairo, Egypt.

2.3. Preparation of green spinach leaves extract

Fresh spinach (*Spinacia oleracea*) leaves were washed several times with running water to get rid of the dust particles, and dried under sunlight to remove the residual moisture. Then, spinach leaves were washed with distilled water for any possible impurity as shown in Figure 1. Typically; in a 250 ml vessel about 10 g of fresh spinach leaves dried up, and cut into very small pieces were added to 100 ml de-ionized water under vigorous stirring, and the reaction temperature was raised to 100 ^{o}C for 30 min. Then, the mixture was naturally cooled, and filtered using Whatman filter paper. The filtrate was centrifuged for 30 min at 4000 rpm and collected and stored at room temperature [26].

2.4. Green synthesis of silver nanoparticles:

Typically, in a 250 ml reaction vessel, an aqueous solution of $AgNO_3$ (1 mM/50 ml) was added to 5 ml of spinach leaves extract under vigorous stirring. The reaction temperature was raised to 90 ºC for 1 hr. The color was changed from light yellow to yellowish-brown after 1 hr indicating the formation of Ag NPs.

Fig.1. Scheme for preparation of spinach (*Spinacia oleracea*) leaves extract.

2.5. Characterization

Optical properties in terms of UV-Vis absorption were obtained using a JASCO 730 double beam spectrophotometer. The absorption spectra were recorded in the range from 200 to 900 nm, with an increment of the wavelength of about 0.2 nm. Transmission Electron Microscope (TEM) JEOL, model 1200EX was used to investigate the micrograph of obtained samples under operating voltage 120 kV. In addition, X-ray diffraction (XRD) measurements have been carried out using an Ultima IV (Rigaku, Japan) Powder Diffractometer operating with a Cu target with Kα1 = 1.54060 Å, in the 2θ range of 20-70 degrees. X-ray scan was performed in 2θ/θ continuous mode at 2 degrees per min, with a step size of 0.02. The tube voltage and tube current were maintained at 40 kV and 40 mA, respectively,

The size distribution and zeta-potential of sterilized AgNPs were measured by Malvern zetasizer Nano ZS instrument with He/Ne laser (633 nm) at an angle of 173° collecting backscatter optics. Furthermore, FT-IR of green synthesized AgNPs was obtained in the range from 400 to 4000 cm^{-1} using JASCO 6700 Fourier transform infrared spectrometer (FT-IR).

2.6. Antimicrobial property.

The silver nanoparticles (AgNPs) synthesized using *Spinacia oleracea* leaves extract was tested for the antimicrobial activity using two different methods standard agar-well diffusion method and broth microdilution assay.

A- Agar well diffusion method.

Klebsiella pneumoniae, Escherichia coli, Acinitobacter baumannii, Pseudomonas aeruginosa, Staphylococcus aureus, and *Staphylococcus haemolyticus*, human pathogenic bacteria were used as the test specimens. Pure cultures of the test specimens were sub-cultured in nutrient broth and the strain was uniformly spread on sterilized petri plates with Muller-Hinton agar. A circular well of 6 mm diameter was made in plates using a sterile cork-borer.

The well was loaded with (50 µl) AgNPs to check the antibacterial activity and the plates were incubated at 37 ºC overnight and the zones of inhibition were measured.

In addition for antifungal activity of AgNPs was examined using agar well diffusion method. *Aspergilus niger*, *Penicillium marneffie, Candida glabrata and Candida parapsilosis* fungal strains were maintained on Czapex Dox Agar (CDA) at 28 °C, and 5-day old cultures were used for antifungal analysis. Three to four mL of sterile normal saline was poured onto the fungal lawns and conidia were collected by gentle scraping. One hundred µl of this liquid spore suspension was evenly spread plated onto fresh Potato Dextrose Agar (PDA) plates. A circular well of 6 mm diameter was made in plates using a sterile cork-borer. The well was loaded with (50 µl) AgNPs to check the antifungal activity and the plates were then incubated for 2-3 days at 28 ºC and the zones of inhibition were measured.

B- Broth microdilution assay.

Suspension equivalent to the turbidity of 0.5 McFarland standard (10^8 CFU/ml) prepared from afresh subculture in Mueller Hinton Broth (MHB) for bacteria and Sabouraud Dextrose Broth (SDB) for fungi/yeast, then the suspension was diluted to 10^6 CFU/ml. The adjusted microbial inoculums (100 µl) were added to each well of sterile flat-bottomed 96-well microtiter plate containing the tested concentration of AgNPs (100 µl/well). As a result, the last inoculum concentration of 5×10^5 CFU/ml was obtained in each well. In the plates, wells containing microbial suspension without tested AgNPs used as growth control for tested microbes and other wells containing only media as a background control were included. Optical densities were measured at 620 nm after 24 hr at 37°C for bacteria and 48 hr at 28°C for fungi/yeast using an ELISA microplate reader (Sunrise™-TECAN, Switzerland) at the national cancer institute Cairo University. Finally, cell concentrations were transformed to a mean growth inhibition percentage (%). The percentage of microbial growth reduction (GR %) was estimated using as reference the control treatment (without extract) as $\mathbf{GR\ \% = \frac{CT}{C} x100}$ Where, *C* is the cell concentrations under the control treatment and *T* is the cell concentrations under the extract treatment. Three replicates were considered. The results were recorded as means ± SE of the triplicate experiment.

2.7. Preparation of Resazurin Solution

The resazurin solution was prepared at 0.02% (Wt/Vol) [27]. A 0.002 g of resazurin salt powder was dissolved in 10 mL of distilled water and vortexed. The mixture was filtered by a Millipore membrane filter (0.2 µm). The solution can be kept at 4°C for 2 weeks.

2.8. Determination of Minimum Inhibitory Concentration (MIC) for bacteria.

The MIC of green synthesized AgNPs was done using the method described in the guideline of CLSI [28]. The MIC test was performed in 96-well round-bottom microtiter plate using standard broth microdilution methods. The bacterial inoculums were adjusted to the concentration of 106 CFU/ml. For the MIC test, 100 µl of the synthesized AgNPs stock solution (256 µg/mL) was added and diluted 2-fold with the bacterial inoculums in 100 µl of MHB started from column 4 to column 12. Column 4 of the microtiter plate contained the highest concentration of AgNPs, while column 12 contained the lowest concentration. Column 1 served as a positive control (medium and bacterial inoculums) and column 2 served as a negative control (only medium). Each well of the microtiter plate was added with 30 µl of the resazurin solution and incubated at 37°C for 24 h. Any color changes were observed. Blue/purple color indicated no bacterial growth while pink/colorless indicated bacterial growth. The MIC value was taken at the lowest concentration of antibacterial agents that inhibits the growth of bacteria (color remained in blue).

2.9. Determination of Minimum Inhibitory Concentration (MIC) for fungi.

Stock inoculum suspensions were prepared in sterile saline (provided by Trek Diagnostic Systems) containing 1% Tween 80 from 7-day-old colonies grown on potato dextrose agar slants (provided by Remel, Lenexa, Kans.). The actual stock inoculum suspensions by inoculum quantification ranged from 0.9×10^6 to 4.5×10^6 CFU/ml for 95% of the inoculum densities evaluated. On the day of the test, each microdilution well containing 100 µl of the diluted (twofold) AgNPs concentrations was inoculated with 100 µl of the diluted (two times) conidial inoculum suspensions in liquid Potato Dextrose Agar (PDA) (final volume in each well 200 µl). The microdilution trays were incubated at 28°C and examined after 4 days of incubation. The MIC endpoints were the lowest AgNPs concentrations that showed absence of growth or complete growth inhibition (100% inhibition). On the other hand, unicellular fungi were treated like bacteria as described above.

2.10. Cytotoxicity assay to evaluate nanoparticles toxicity by using tissue culture.

According to Riss and Moravec [29] by using (MTT protocol) the 96 well tissue culture plate was inoculated with 1×10^5 cells/ml (100 ul/well) and incubated at 37 °C for 24 hours to develop a complete monolayer sheet. growth medium was decanted from 96 well microtiter plates after confluent sheet of cells were formed, the cell monolayer was washed twice with wash media (two-fold dilution) was made in medium with 2% serum (maintenance medium) 0.1 ml of each dilution was tested in different wells leaving 3 wells as control, receiving only maintenance medium. The plate was incubated at 37 °C then examined. Cells were checked for any physical signs of toxicity such as (partial or complete loss of monolayer, rounding, Shrinkage, or cell granulation). 20ul MTT solution was added to each well then placed on a shaking table at 150 rpm for 5 minutes to thoroughly mix the MTT into the media then incubated (37 °C and 5% CO_2) for 1-5hours to allow the MTT to be metabolized then dumbed off the media, dried plate towels to remove residue if necessary, resuspended formazan (MTT metabolic product) in 200ul DMSO then placed on a shaking table at 150 rpm for 5 minutes to thoroughly mix the formazan into the solvent finally, optical density values were recorded at wavelength 560 nm and subtract background at 620nm which optical density should be directly correlated with cell quantity.

3. Results and discussion

3.1. Synthesis and characterization of green-synthesized silver nanoparticles

Silver nanoparticles were green synthesized using Spanish leaf extract. In this process, the formation of silver nanoparticles (AgNPs) is identified through the color change during the reaction processes. In our case, the color change from the light yellow to a yellowish-brown color indicating to the reduction of silver ions (Ag^{1+}) to zero valent silver particles (Ag^0).

Such case, the Spanish leaf extract has a dual function, which acts as both reducing and stabilizing agents as a result of existence for some chemical compound such as alkaloids, flavonoids, saponins, steroids. Moreover, the formation of the biosynthesized AgNPs was confirmed by UV-Vis spectroscopy measurements. Figure 2 shows a broad absorption band located around 410 nm indicating to the formation of AgNPs.

In addition, a shoulder at 320 nm is associated with UV-Vis spectrum that owing to formation of Ag nanoclusters. This beak, due to the surface plasmon resonance typical of AgNPs and indicates that the particles were well dispersed without aggregation [30-32]. The morphological and structural properties of the as-prepared AgNPs were confirmed by using TEM and XRD as shown in Figs. 3 and 4, respectively.

TEM micrograph shows that AgNPs are quasi-spherical without any agglomeration and with polydispersity distribution. The average particle size was about 15±5 nm Figure 3. The result is comparable with the *A. nilagirica* leaf extract-mediated silver nanoparticles [33].

XRD patterns as depicted in Figure 4 display a two strong and narrow reflection at the position of around 2θ 38.78°, suggesting the lattice-spacing distance (d_{hkl}) of 2.35 Å, which reveals to (111) crystallographic reflection of the face-centered cubic structure (fcc) of Ag atom. The second one is at 2θ 65.14°, suggesting the lattice-spacing distance (d_{hkl}) of 1.45 Å, which reveals to (220) crystallographic reflection of the face-centered cubic structure (fcc) of the Ag atom [4].

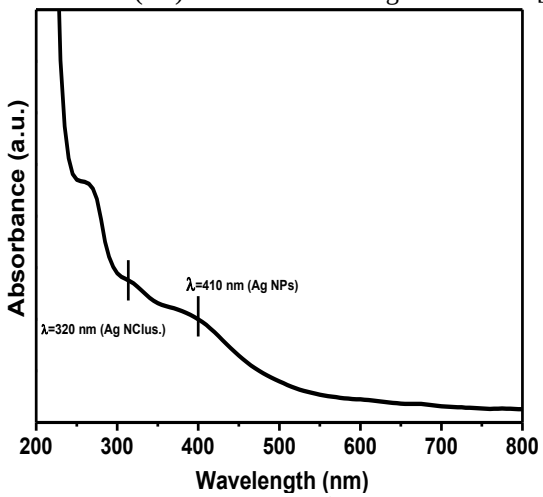

Fig.2. UV-Vis absorption spectra of green synthesized AgNPs using spinach (*S. oleracea*) leaves extract.

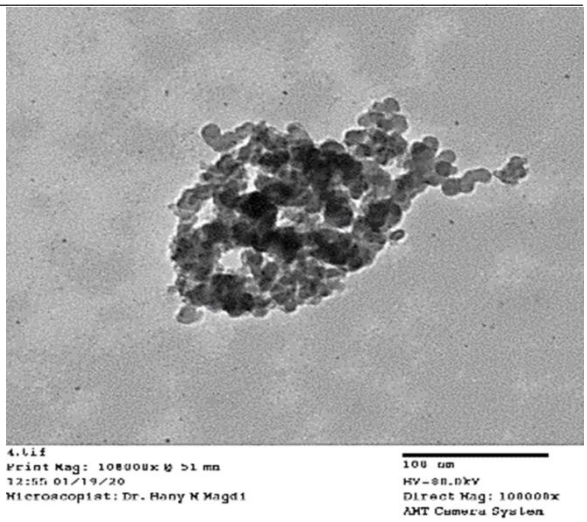

Fig.3. TEM micrographs of green synthesized AgNPs using spinach (*S. oleracea*) leaves extract.

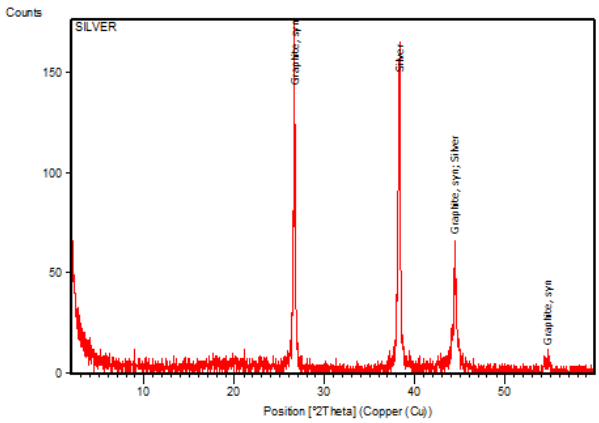

Fig.4. XRD patterns of green synthesized AgNPs using spinach (*S. oleracea*) leaves extract.

Furthermore, the colloidal stability of AgNPs has been investigated using the dynamic light scattering (DLS) technique, and zeta-potential measurements as shown in Figure 5. The hydrodynamic diameter (H_D) for as-prepared AgNPs in a vehicle solution was about 15.19 ± 1.107 nm with a polydispersity index (PDI) 0.349, which indicated the narrow distribution of the AgNPs [34], as shown in (Figure 5a). Whereas, the zeta-potential (η) of as-prepared AgNPs by Spanish leaf extract was about -43.1±3.73 mV (Figure 5b). The negative value indicated the stability of the nanoparticles and it evaded the agglomeration of nanoparticles [35, 36]. The negative potential value might be due to the capping action of biomolecules present in the leaf extract of *S. oleracea*.

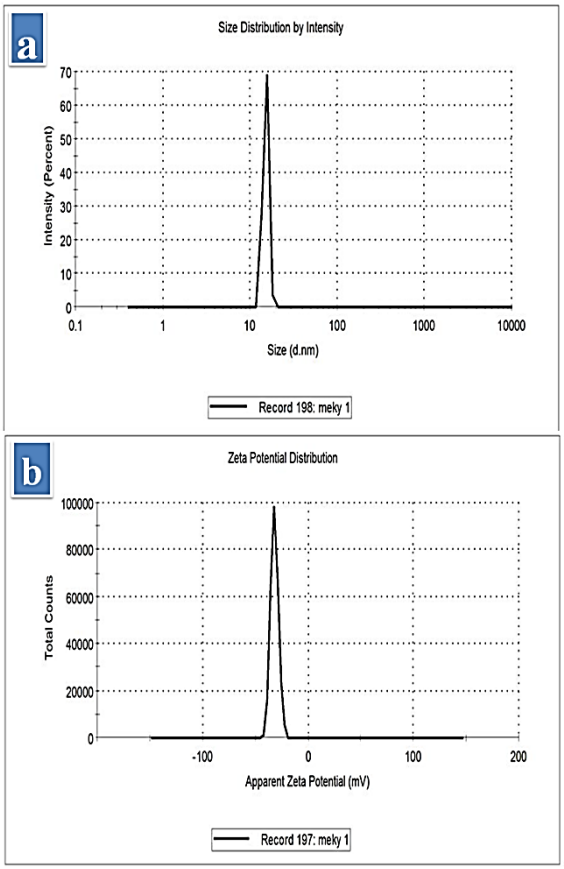

Fig.5. (**a**) DLS and (**b**) Zeta-potential data for green synthesized AgNPs using spinach (*S. Oleracea*) leaves extract.

Finally, FT-IR showed the same strong stretching bands at wavenumbers of 2526.3 and 3031 cm^{-1} due to the presence of –OH (hydroxyl group) and –NH (amine salt), respectively, exist in PVP molecules (Figure 6).

FT-IR analysis was carried out to identify the possible interactions between silver and bioactive molecules, which may be responsible for the synthesis and stabilization (capping) of AgNPs (Figure 6). The intense peak 3435, 2085, 1639, 1369, 1226, and 532 cm^{-1} indicated the presence of hydroxyl (OH) group, benzene ring, carboxylic (C=O) group, alkyl halide group respectively.

The results of the FT-IR were used to identify the possible biomolecules responsible for the stabilization of the synthesized silver nanoparticles. The prominent peaks of the FT-IR results are showing the corresponding values to the amide group (N-H stretching 3435 cm^{-1}), alkane group (CH-2085 cm^{-1}) alkene (CC- 1639, 1369, 1226, and 532 cm^{-1}) and ether groups (COC- 1031.73 cm^{-1}). Similar observation also found as flavonoids, triterpenoids and poly phenols [37].

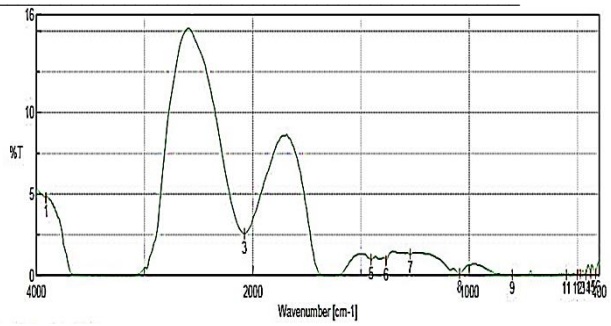

Fig.6. FT-IR spectra for green synthesized AgNPs using spinach (*S. oleracea*) leaves extract.

Hence, the terpenoids are proved to have the good potential activity to convert the aldehyde groups to carboxylic acids in the metal ions. Further, amide groups are also responsible for the presence of the enzymes and these enzymes are responsible for the reduction synthesis and stabilization of the metal ions, further, polyphenols are also proved to have a potential reducing agents in the synthesis of the AgNPs [38].

3.2. Antimicrobial property (antibacterial and antifungal activity)

The antimicrobial property of silver is well-known for many years. The antimicrobial property including the antibacterial activity of the green synthesized AgNPs has been investigated on *Klebsiella pneumoniae, Escherichia coli, Acinitobacter baumannii, Pseudomonas aeruginosa, Staphylococcus haemolyticus,* and *Staphylococcus aureus* as bacterial strains (Figures 7 and 8) in addition, the antifungal activity on *Aspergilus niger*, *Penicillium maeneffie, Candida glabrata and Candida parapsilosis* as a fungal strains (Figures 9and 10) [39].

Regarding the antibacterial activity of AgNPs, the result of the well diffusion method revealed that AgNPs inhibit the bacterial growth of the tested strains (*Klebsiella pneumonia*, *Escherichia coli, Acinitobacter baumannii*, *Pseudomonas aeruginosa, Staphylococcus aureus,* and *Staphylococcus haemolyticus*) at an appropriate volume of 50µl of green synthesized AgNPs solution.

The inhibition zones of the samples are compared with a pure medium as a positive control and de-ionized water as a negative control, and the obtained zone indicates the antimicrobial activity of AgNPs. Based on the obtained results, *Staphylococcus haemolyticus* was found to be more

susceptible to AgNPs with an inhibition zone diameter of 34 mm. This result might be due to the activity of particles in this experiment, depending on the direct contact of a particle with bacteria**.**

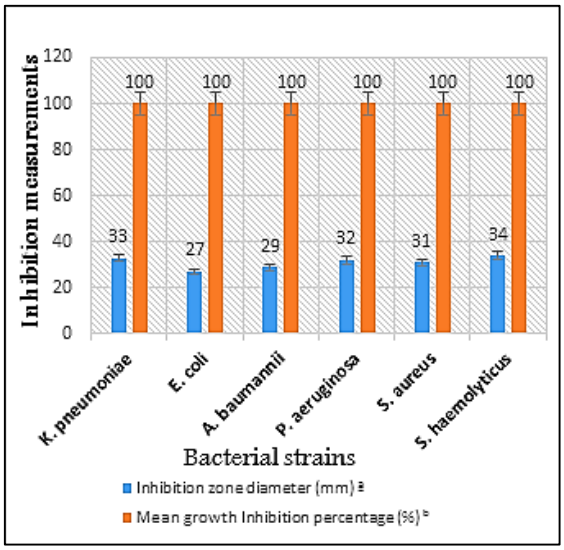

Fig.7. Antibacterial activity histogram of AgNPs (50 µl) against the pathogenic bacterial strains using inhibition zone diameter and mean growth inhibition percentage.

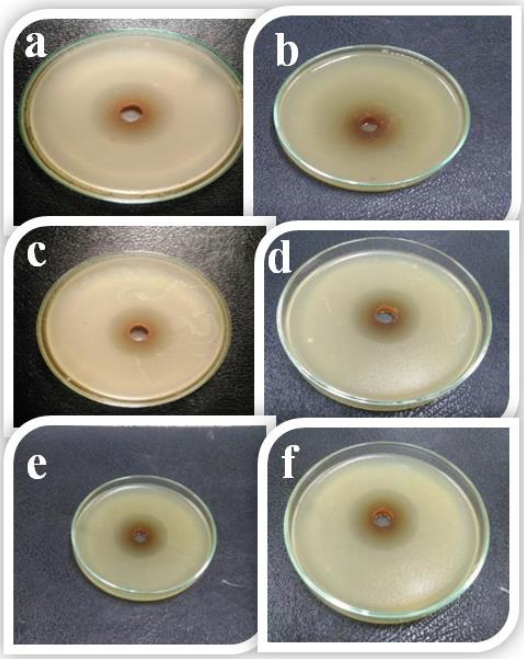

Fig.8. Inhibition zones produced against tested bacterial strains (a) *K. pneumoniae*, (b) *E. coli*, (c) *A. baumannii*, (d) *P. aeruginosa*, (e) *S. aureus* and (f) *S. haemolyticus* using Synthesizing silver nanoparticles (50 µl).

Regarding the antifungal activity of as-prepared AgNPs against *Aspergilus niger*, *Penicillium maeneffie, Candida glabrata* and *Candida parapsilosis* as tested fungal strains have been investigated using the well diffusion method.

The results as shown in Figures 9 and 10 showed that *Aspergilus niger* is to be more susceptible to AgNPs than other fungal isolates with an inhibition zone of about 39 mm at an appropriate volume of 50 µl of as-prepared AgNPs solution.

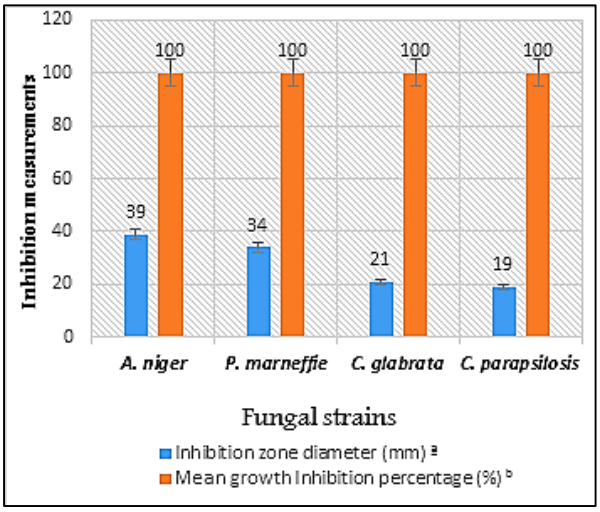

Fig.9. Antifungal activity histogram of AgNPs (50 µl) against the pathogenic fungal strains using inhibition zone diameter and mean growth inhibition percentage.

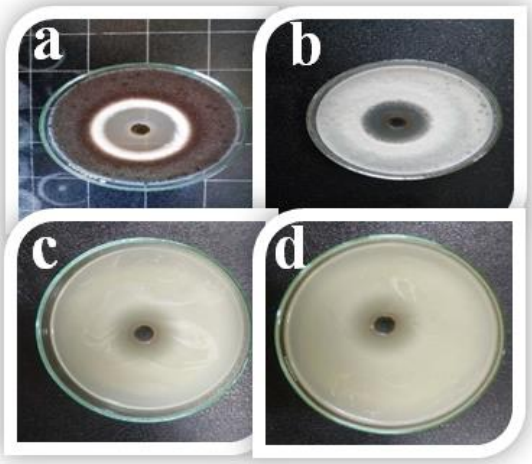

Fig.10. Inhibition zones produced against (a) *A. niger*, (b) *P. marneffie*, (c) *C. glabrata* and (d) *C. parapsilosis* using green synthesized silver nanoparticles (AgNPs) (50 µl).

3.3. Determination of minimum inhibitory concentration (MIC)

Minimum inhibitory concentration (MIC) values of Ag NPs against the multidrug-resistant bacteria were ranged from 4 to 8 µg/ml (Figure 11). *K. pneumonia, A. baumanni, P. aeruginosa, S. aureus,* and *S. haemolticus* showed the MIC value of 4 µg/mL, while *E. coli* showed the MIC value of 8 µg/ml. In another study, the MIC values of AgNPs

against the foodborne pathogens were ranged from 3.9 to 7.8 µg/mL. *K. pneumonia* showed the MIC value of 3.9 µg/ml while *E. coli* showed the MIC value of 7.8 µg/mL [40]**.** The MIC value of *E.coli* showed that *E.coli* was less susceptible to AgNPs. This may due to the positive charges of AgNPs trapped and blocked by lipopolysaccharide, thus make *E. coli* less susceptible to AgNPs [41].

Resazurin dye was used in the study as an indicator in the determination of cell growth, especially in cytotoxicity assays [42]. Oxidoreductases within viable cells reduced the resazurin salt to resorufin and changed the color from blue non-fluorescent to pink and fluorescent (Figure 11). While the determination of MIC for AgNPs against the fungal strains has been dipeicated in Figure 12. The potential antifungal activity of AgNPs *C. parapsilosis*, and *C. glabrata* was confirmed by MIC testing. The MIC of silver nanoparticles of all *Candida* species tested was 8 µg/ml Figure 12. No inhibition was observed in the low concentration range (2 to 4 µg/mL), but growth was significantly inhibited at 8 µg/ml or more compared to the control (Figure 12).

Fig.11. Plates of the colorimetric-XTT assay for determination of MIC values of AgNPs against bacterial strains using resazurin salt, (1) cart preparation, (2) after addition resazurin dye and (3) the results after incubation.

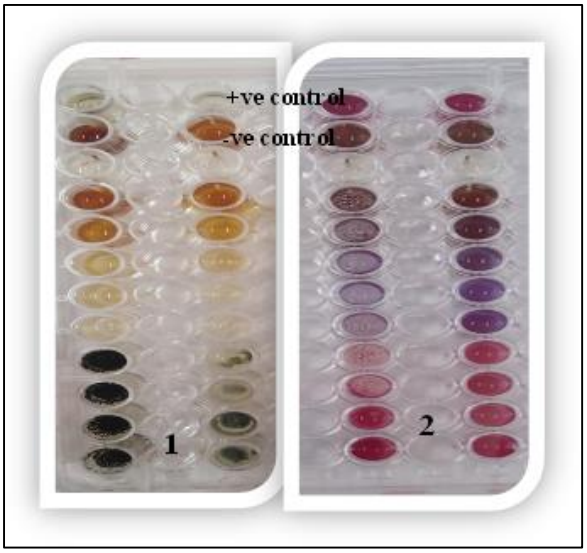

Fig.12. Plates of the colorimetric-XTT assay for determination of MIC values of AgNPs against fungal strains using resazurin salt.

3.4. Cytotoxicity assay

The cell viability assay is one of the important methods for toxicology analysis that explain the cellular response to toxic materials, and it can provide information on cell death, survival, and metabolic activities [43]. AgNPs treated cells showed the decreased metabolic activity, which depends on the nature of cell types and size of nanoparticles. Others reported that colloidal silver induced a dose-dependent cytotoxic effect on MCF-7 and MDA-MB-231 breast cancer cells [44, 45]. In our experiment, the cells were treated with various concentrations (31.25–1000 µg/mL) of AgNPs for 24 h, and the results suggest that AgNPs were able to reduce the cell viability of Wi38 cells in a dose-dependent manner. In our study at 24 h of treatment of lung tissue, AgNPs were found to be cytotoxic to the cells at concentrations of 500 µg/mL and higher. Our results suggest that the known concentration of AgNPs significantly inhibits the growth of cells. The results corresponding to the cytotoxicity test show slight differences in cell viability between 24 and 48 hr. of cell exposition to AgNPs. It is possible to observe toxicity for silver nanoparticles at the highest concentrations used (Figure 13). AshaRani ***et al***. [42] report similar results for lung fibroblasts in response to silver NPs exposition, arguing a cytotoxicity dependence on NPs concentration as well as cell-cycle detection. Additionally, Ahmad *et al.* [46] evaluated the effect of silver and gold nanoparticles obtained by the green synthesis method in murine

macrophages using concentrations in the range of 10–1000 µg /mL, obtaining less cytotoxicity at a concentration lower than 80 µg/mL. Corresponding to the fluorescence microscopy analysis, it was observed that, at a lower concentration of treatments, there was more confluence and cell density compared to the control group (Figure 13). On the other hand, as concentrations increased, alterations in cell morphology and few cell extensions were observed [1, 47].

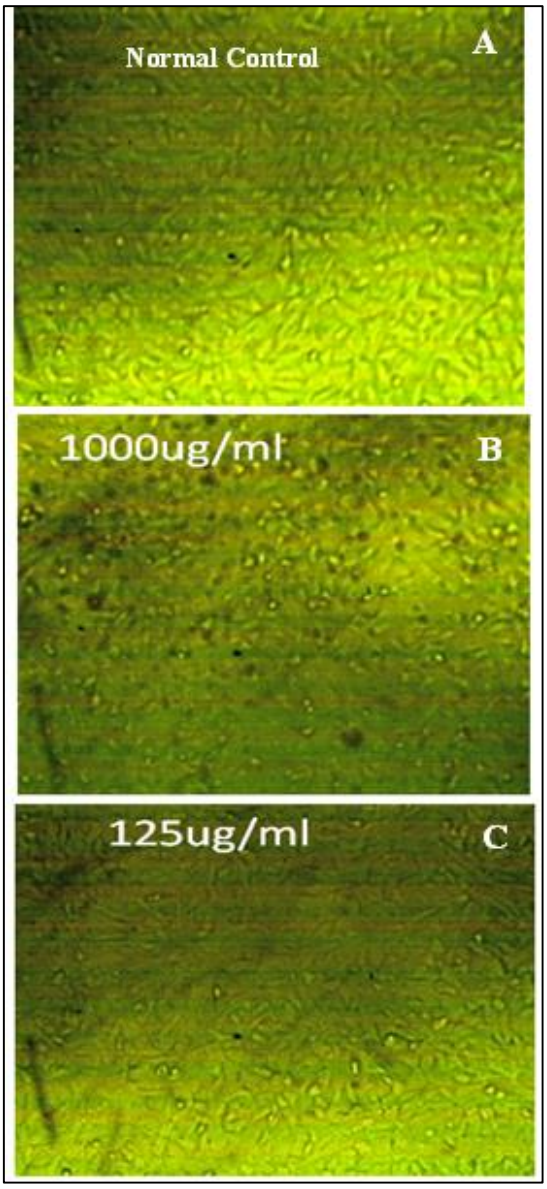

Fig.13. Effect of AgNPs on wi38 Homo sapiens, lung, fibroblast, adherent and normal) cells at different concentrations. (A) Normal cells, (B) the effect at 1000 ug/mL, (C) the effect at 125 ug/mL.

4. Conclusions

In this study, biocompatible green-synthesized AgNPs were prepared through a non-toxic and eco-friendly green chemical route using fresh spinach (*Spinacia oleracea*) leaf extract. The physical properties of the as-prepared AgNPs were investigated via different characterization techniques such as UV-Vis optical absorption, a morphological structure using TEM, and XRD. In addition, the colloidal stability using zeta sizer technique and surface functionality using FT-IR spectroscopy. The average particle size was about 15±5 nm. Furthermore, the as-prepared particles showed significant antimicrobial activity against different MDR-bacterial and fungal isolates. Silver nanoparticles synthesized by this method are very useful in many versatile applications. Such nanoparticles produced from *Spinacia oleracea* extract without any toxic chemical reagents have many advantages, including simple production, cost-effectiveness, eco-friendly fabrication and product, and biocompatibility. These properties will enable AgNPs to be used in diverse areas. Specifically, the application of AgNPs to bactericidal and fungicidal therapy may make a considerable contribution to nanomedicine.

Conflicts of interest

There are no conflicts to declare.

5. References

[1] S.M. Alsharif, S.S. Salem, M.A. Abdel-Rahman, A. Fouda, A.M. Eid, S. El-Din Hassan, M.A. Awad, A.A. Mohamed, Multifunctional properties of spherical silver nanoparticles fabricated by different microbial taxa, Heliyon, 6 (2020).

[2] G. Zhang, S. Sun, M.N. Banis, R. Li, M. Cai, X. Sun, Morphology-Controlled Green Synthesis of Single Crystalline Silver Dendrites, Dendritic Flowers, and Rods, and Their Growth Mechanism, Crystal Growth & Design, 11 (2011) 2493-2499.

[3] M. Abu-Elghait, M. Hasanin, A.H. Hashem, S.S. Salem, Ecofriendly novel synthesis of tertiary composite based on cellulose and myco-synthesized selenium nanoparticles: Characterization, antibiofilm and biocompatibility, International Journal of Biological Macromolecules, 175 (2021) 294-303.

[4] M.S. Aref, S.S. Salem, Bio-callus synthesis of silver nanoparticles, characterization, and antibacterial activities via Cinnamomum

camphora callus culture, Biocatalysis and Agricultural Biotechnology, 27 (2020).

[5] A.M. Eid, A. Fouda, G. Niedbała, S.E.D. Hassan, S.S. Salem, A.M. Abdo, H.F. Hetta, T.I. Shaheen, Endophytic streptomyces laurentii mediated green synthesis of Ag-NPs with antibacterial and anticancer properties for developing functional textile fabric properties, Antibiotics, 9 (2020) 1-18.

[6] A.H. Hashem, A.M.A. Khalil, A.M. Reyad, S.S. Salem, Biomedical Applications of Mycosynthesized Selenium Nanoparticles Using Penicillium expansum ATTC 36200, Biological Trace Element Research, (2021).

[7] T.I. Shaheen, A. Fouda, S.S. Salem, Integration of Cotton Fabrics with Biosynthesized CuO Nanoparticles for Bactericidal Activity in the Terms of Their Cytotoxicity Assessment, Industrial and Engineering Chemistry Research, 60 (2021) 1553-1563.

[8] A. Singh, P.K. Gautam, A. Verma, V. Singh, P.M. Shivapriya, S. Shivalkar, A.K. Sahoo, S.K. Samanta, Green synthesis of metallic nanoparticles as effective alternatives to treat antibiotics resistant bacterial infections: A review, Biotechnology Reports, 25 (2020) e00427.

[9] A.A. Mohamed, M. Abu-Elghait, N.E. Ahmed, S.S. Salem, Eco-friendly Mycogenic Synthesis of ZnO and CuO Nanoparticles for In Vitro Antibacterial, Antibiofilm, and Antifungal Applications, Biological Trace Element Research, (2020).

[10] M.A. Elbahnasawy, A.M. Shehabeldine, A.M. Khattab, B.H. Amin, A.H. Hashem, Green biosynthesis of silver nanoparticles using novel endophytic Rothia endophytica: Characterization and anticandidal activity, Journal of Drug Delivery Science and Technology, 62 (2021) 102401.

[11] S.S. Salem, A. Fouda, Green Synthesis of Metallic Nanoparticles and Their Prospective Biotechnological Applications: an Overview, Biological Trace Element Research, 199 (2021) 344-370.

[12] S. Elsawy, W.M. Elsherif, R. Hamed, Effect of silver nanoparticles on vancomycin resistant Staphylococcus aureus infection in critically ill patients, Pathogens and Global Health, (2021) 1-10.

[13] E. Abbasi, M. Milani, S. Fekri Aval, M. Kouhi, A. Akbarzadeh, H. Tayefi Nasrabadi, P. Nikasa, S.W. Joo, Y. Hanifehpour, K. Nejati-Koshki, M. Samiei, Silver nanoparticles: Synthesis methods, bio-applications and properties, Critical Reviews in Microbiology, 42 (2016) 173-180.

[14] B. Ahmed, A. Hashmi, M.S. Khan, J. Musarrat, ROS mediated destruction of cell membrane, growth and biofilms of human bacterial pathogens by stable metallic AgNPs functionalized from bell pepper extract and quercetin, Advanced Powder Technology, 29 (2018) 1601-1616.

[15] F. Paladini, M. Pollini, A. Tala, P. Alifano, A. Sannino, Efficacy of silver treated catheters for haemodialysis in preventing bacterial adhesion, Journal of Materials Science: Materials in Medicine, 23 (2012) 1983-1990.

[16] K.B. Narayanan, N. Sakthivel, Green synthesis of biogenic metal nanoparticles by terrestrial and aquatic phototrophic and heterotrophic eukaryotes and biocompatible agents, Advances in Colloid and Interface Science, 169 (2011) 59-79.

[17] S. Kumar, S. Jain, M. Nehra, N. Dilbaghi, G. Marrazza, K.-H. Kim, Green synthesis of metal–organic frameworks: A state-of-the-art review of potential environmental and medical applications, Coordination Chemistry Reviews, 420 (2020) 213407.

[18] S. Ahmed, M. Ahmad, B.L. Swami, S. Ikram, A review on plants extract mediated synthesis of silver nanoparticles for antimicrobial applications: A green expertise, Journal of Advanced Research, 7 (2016) 17-28.

[19] S.S. Salem, E.F. El-Belely, G. Niedbała, M.M. Alnoman, S.E.D. Hassan, A.M. Eid, T.I. Shaheen, A. Elkelish, A. Fouda, Bactericidal and in-vitro cytotoxic efficacy of silver nanoparticles (Ag-NPs) fabricated by endophytic actinomycetes and their use as coating for the textile fabrics, Nanomaterials, 10 (2020) 1-20.

[20] L. Huang, Y. Sun, S. Mahmud, H. Liu, Biological and environmental applications of silver nanoparticles synthesized using the aqueous extract of Ginkgo biloba leaf, Journal of Inorganic and Organometallic Polymers and Materials, 30 (2020) 1653-1668.

[21] A.A. Mohmed, A. Fouda, M.S. Elgamal, S. El-Din Hassan, T.I. Shaheen, S.S. Salem, Enhancing of cotton fabric antibacterial properties by silver nanoparticles synthesized by new egyptian strain fusarium keratoplasticum A1-3, Egyptian Journal of Chemistry, 60 (2017) 63-71.

[22] Y.-G. Yuan, Q.-L. Peng, S. Gurunathan, Effects of silver nanoparticles on multiple drug-resistant strains of Staphylococcus aureus and Pseudomonas aeruginosa from mastitis-infected goats: an alternative approach for antimicrobial therapy, International journal of molecular sciences, 18 (2017) 569.

[23] M.R. Shaik, M. Khan, M. Kuniyil, A. Al-Warthan, H.Z. Alkhathlan, M.R.H. Siddiqui, J.P. Shaik, A. Ahamed, A. Mahmood, M. Khan, Plant-extract-assisted green synthesis of silver nanoparticles using Origanum vulgare L. extract and their microbicidal activities, Sustainability, 10 (2018) 913.

[24] F. Erci, R. Cakir-Koc, I. Isildak, Green synthesis of silver nanoparticles using Thymbra spicata L. var. spicata (zahter) aqueous leaf extract and evaluation of their morphology-dependent antibacterial and cytotoxic activity, Artificial cells, nanomedicine, and biotechnology, 46 (2018) 150-158.

[25] P. Vos, G. Garrity, D. Jones, N.R. Krieg, W. Ludwig, F.A. Rainey, K.-H. Schleifer, W.B. Whitman, Bergey's manual of systematic bacteriology: Volume 3: The Firmicutes, Springer Science & Business Media, 2011.

[26] S.U. Rahman, K. Sultana, Green synthesis of silver nanoparticles using Spinacia oleracea leave extract and their physical verification, Gomal University Journal of Research, 33 (2017) 91-101.

[27] R.A. Khalifa, M.S. Nasser, A.A. Gomaa, N.M. Osman, H.M. Salem, Resazurin Microtiter Assay Plate method for detection of susceptibility of multidrug resistant Mycobacterium tuberculosis to second-line anti-tuberculous drugs, Egyptian Journal of Chest Diseases and Tuberculosis, 62 (2013) 241-247.

[28] F.R. Cockerill, Performance standards for antimicrobial susceptibility testing, Approved Standard M100-S20, (2010).

[29] T.L. Riss, R.A. Moravec, Use of multiple assay endpoints to investigate the effects of incubation time, dose of toxin, and plating density in cell-based cytotoxicity assays, Assay and drug development technologies, 2 (2004) 51-62.

[30] A. Fouda, A. Mohamed, M.S. Elgamal, S. EL-Din Hassan, S. Salem Salem, T.I. Shaheen, Facile approach towards medical textiles via myco-synthesis of silver nanoparticles, Der Pharma Chemica, 9 (2017).

[31] A.A. Mohmed, E. Saad, A. Fouda, M.S. Elgamal, S.S. Salem, Extracellular biosynthesis of silver nanoparticles using Aspergillus sp. and evaluation of their antibacterial and cytotoxicity, Journal of Applied Life Sciences International, (2017) 1-12.

[32] C. Krishnaraj, E.G. Jagan, S. Rajasekar, P. Selvakumar, P.T. Kalaichelvan, N. Mohan, Synthesis of silver nanoparticles using Acalypha indica leaf extracts and its antibacterial activity against water borne pathogens, Colloids and Surfaces B: Biointerfaces, 76 (2010) 50-56.

[33] M. Vijayakumar, K. Priya, F.T. Nancy, A. Noorlidah, A.B.A. Ahmed, Biosynthesis, characterisation and anti-bacterial effect of plant-mediated silver nanoparticles using Artemisia nilagirica, Industrial Crops and Products, 41 (2013) 235-240.

[34] H.R. Ghorbani, Biosynthesis of silver nanoparticles using Salmonella typhirium, Journal of Nanostructure in Chemistry, 3 (2013) 29.

[35] S.V. Patil, H.P. Borase, C.D. Patil, B.K. Salunke, Biosynthesis of Silver Nanoparticles Using Latex from Few Euphorbian Plants and Their Antimicrobial Potential, Applied Biochemistry and Biotechnology, 167 (2012) 776-790.

[36] J.J. Antony, M.A.A. Sithika, T.A. Joseph, U. Suriyakalaa, A. Sankarganesh, D. Siva, S. Kalaiselvi, S. Achiraman, In vivo antitumor activity of biosynthesized silver nanoparticles using Ficus religiosa as a nanofactory in DAL induced mice model, Colloids and Surfaces B: Biointerfaces, 108 (2013) 185-190.

[37] A. Nabikhan, K. Kandasamy, A. Raj, N.M. Alikunhi, Synthesis of antimicrobial silver nanoparticles by callus and leaf extracts from saltmarsh plant, Sesuvium portulacastrum L, Colloids and Surfaces B: Biointerfaces, 79 (2010) 488-493.

[38] T. Prasad, E. Elumalai, Biofabrication of Ag nanoparticles using Moringa oleifera leaf extract and their antimicrobial activity, Asian Pacific Journal of Tropical Biomedicine, 1 (2011) 439-442.

[39] Y.Y. Loo, Y. Rukayadi, M.-A.-R. Nor-Khaizura, C.H. Kuan, B.W. Chieng, M. Nishibuchi, S. Radu, In vitro antimicrobial activity of green synthesized silver nanoparticles against selected gram-negative foodborne pathogens, Frontiers in microbiology, 9 (2018) 1555.

[40] H.H. Lara, N.V. Ayala-Núñez, L.d.C. Ixtepan Turrent, C. Rodríguez Padilla, Bactericidal effect of silver nanoparticles against multidrug-resistant bacteria, World Journal of Microbiology and Biotechnology, 26 (2010) 615-621.

[41] B.P. McNicholl, J.W. McGrath, J.P. Quinn, Development and application of a resazurin-based biomass activity test for activated sludge plant management, Water Research, 41 (2007) 127-133.

[42] P.V. AshaRani, G. Low Kah Mun, M.P. Hande, S. Valiyaveettil, Cytotoxicity and Genotoxicity of Silver Nanoparticles in Human Cells, ACS Nano, 3 (2009) 279-290.

[43] X.-l. Song, B. Li, K. Xu, J. Liu, W. Ju, J. Wang, X.-d. Liu, J. Li, Y.-f. Qi, Cytotoxicity of water-soluble mPEG-SH-coated silver nanoparticles in HL-7702 cells, Cell Biology and Toxicology, 28 (2012) 225-237.

[44] S. Gurunathan, J.W. Han, A.A. Dayem, V. Eppakayala, J.H. Park, S.-G. Cho, K.J. Lee, J.-H. Kim, Green synthesis of anisotropic silver nanoparticles and its potential cytotoxicity in human breast cancer cells (MCF-7), Journal of Industrial and Engineering Chemistry, 19 (2013) 1600-1605.

[45] S. Gurunathan, J.W. Han, V. Eppakayala, M. Jeyaraj, J.-H. Kim, Cytotoxicity of biologically synthesized silver nanoparticles in MDA-MB-231 human breast cancer cells, BioMed research international, 2013 (2013).

[46] A. Ahmad, F. Syed, A. Shah, Z. Khan, K. Tahir, A.U. Khan, Q. Yuan, Silver and gold nanoparticles from Sargentodoxa cuneata: synthesis, characterization and antileishmanial activity, RSC Advances, 5 (2015) 73793-73806.

[47] P. Asharani, M.P. Hande, S. Valiyaveettil, Anti-proliferative activity of silver nanoparticles, BMC cell biology, 10 (2009) 1-14.